

## High-Confinement NBI Discharges in W7-AS

U. Stroth, M. Anton, J. Baldzuhn, R. Burhenn, M. Francés<sup>1)</sup>, J. Geiger, T. Geist, L. Giannone, H. Hartfuß, M. Hirsch, R. Jänicke, J.P.T. Koponen, M. Kick, G. Kühner, F.-P. Penningfeld, F. Wagner, A. Weller

Max-Planck-Institut für Plasmaphysik, EURATOM Association, D-85748 Garching,  
<sup>1)</sup>EURATOM-CIEMAT Association, Madrid, Spain

**Abstract:** In W7-AS, the longest energy confinement times were achieved in NBI-heated discharges under low wall-recycling conditions. Low recycling is needed to control the density at line averaged values of  $\bar{n}_e \approx 10^{20} \text{ m}^{-3}$ . Under these conditions, electron and ion temperatures of up to 1 keV and confinement times of 55 ms were obtained with an absorbed heating power of  $P \approx 0.35 \text{ MW}$ . In NBI discharges without density control, the density rose up to typically  $2 \times 10^{20} \text{ m}^{-3}$  and the temperatures remained at 0.3 keV only.

From the H-mode, where after a fast transition the profiles broaden, these discharges can be distinguished by low edge densities and a rather gradual improvement of energy confinement. The reduction of transport is concentrated to a layer at about 2/3 of the plasma radius. In this region steep temperature gradients and a strong gradient in the radial electric field develop. In this respect the discharges are similar to discharges with stronger NBI and additional electron cyclotron resonance heating (ECH), where the highest ion temperatures were achieved [1].

What is specific for the discharges here is the gradual transition. Since the measured electric field is consistent with the neoclassical ambipolar field, this high-confinement mode could be an example where the neoclassical electric field leads to a suppression of anomalous transport, this in turn produces steeper gradients which lead according to neoclassical theory again to a stronger field. This loop is interrupted when transport reaches the neoclassical level. The result is a transport barrier similar as in high performance tokamak discharges like in JET [2].

**Global Energy Confinement Time:** In Fig. 1, we compare the energy confinement time  $\tau_E$  of high-confinement discharges with the W7-AS dataset contributed to the ISS95 scaling [3], which covers our previously accessible parameter range. In the ISS95 dataset a trend was already observed of the kinetic confinement times, as deduced from profiles, being about 15% higher than the diamagnetic ones, for the discharges here, the kinetic confinement time is about 35% higher than the diamagnetic one. A 15% discrepancy can be understood in terms of the diamagnetic loop picking up a component of the vertical field generated by Pfirsch-Schlüter currents. The 35% difference remains unclear at the moment. Since the profiles are well documented for

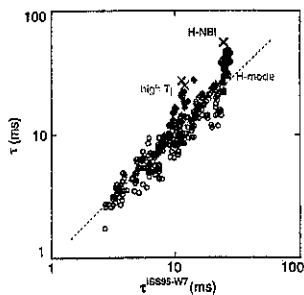


Fig. 1: Diamagnetic confinement times of high-confinement NBI, high ion temperature and H-mode discharges compared with the ISS95 scaling (W7-AS pre-factor) and W7-AS data contributed to the ISS95 database (open symbols). Crosses: kinetic values.

these discharges, we have added the kinetic confinement times to the plot. The figure underlines that the confinement time of these discharges is a factor of 2 above our standard confinement level.

**Characteristics:** In Fig. 2, the main characteristics of a high-confinement NBI discharge are depicted. The distinct feature is the continuous increase from 0.25 to 0.4 s of the energy content at constant heating power and line density. During this phase, which corresponds to three energy confinement times, electron and ion temperatures increase. Simultaneously, a reduction in the  $H_\alpha$  light indicates improving particle confinement. The slow increase of the impurity content in the core is consistent with impurity transport studies [4] yielding a very low particle diffusivity of  $0.07 \text{ m}^2/\text{s}$  and inward convection of  $\delta r/a$  (m/s).

The improvement is accompanied by a reduction in the density fluctuation amplitude, which is partly due to the fact that the reflecting layer moves 1.5 cm inward during the measurement. We observe the reduction primarily in the frequency range below 60 kHz. The radial electric field at a location close to the minimum of the thermal diffusivity becomes continuously stronger while confinement is improving.

In Fig. 3, the temporal evolution of electron density and temperature profiles of this discharge can be studied. The increase of the electron temperature over the entire cross-section and stops at around 0.4 s first in the outer region and later in the core. The increase of the energy content can be partly attributed to the broadening of the profile. The evolution of the density profile continues up to 0.55 s. After an initial evolution from a broad to a more peaked profile, it is primarily the edge density which continues to decrease. We see that a continuing reduction of the edge density does not lead to a further improvement of energy confinement. The possibility of controlling the density seems to be the crucial element rather than the low edge density. Radial derivatives of the data in Fig. 3 show a pronounced steepening of both temperature and density gradients in the radial zone between 10 and 14 cm during the initial phase where confinement improves. The gradients remain unchanged after 0.4 s. The bolometric

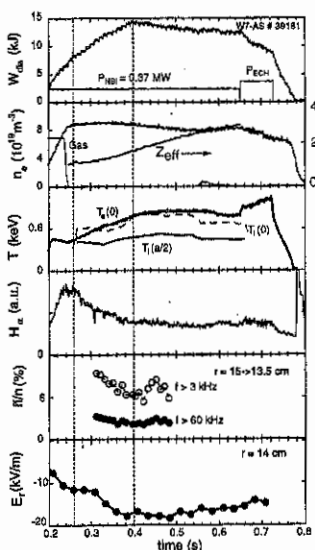


Fig. 2: Time traces of discharge 39181: Diamagnetic energy content and heating power, line averaged density and  $Z_{eff}$  from soft X-ray emission, electron temperature from ECE and ion temperature from a neutral particle analyzer,  $H_\alpha$  light from a limiter, density fluctuation amplitudes from reflectometry integrated over the entire spectrum and over higher frequencies only, radial electric field from passive charge-exchange spectroscopy.

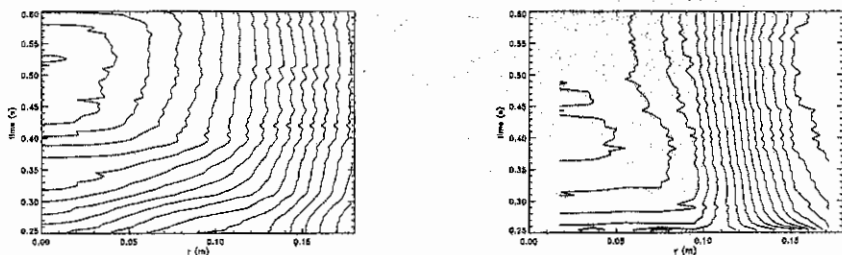


Fig. 3: Temporal evolution of the electron temperature profile from fits to 24 ECE radiometer channels (left) and the density profile unfolded from 8 interferometer channels (right).

radiation profiles are hollow with a maximum at about 0.14 m and start slowly to fill up in the center. At the end of the discharge, this process is not yet completed.

**Power Balance Analyses:** The transport properties of a high-confinement NBI discharge are compared with those of an ECH discharge at similar density and a heating power of 0.5 MW. The ECH discharge serves as "normal" confinement case. Although the absorbed power is higher, the kinetic energy content is only 13 kJ compared to 17 kJ of the NBI discharge. The power balance analyses shown in Fig. 4 were carried out with the same heat diffusivity  $\chi \equiv \chi_e = \chi_i$  for electrons and ions. Electron temperature and density profiles from Thomson scattering serve as input and  $\chi$  as well as the ion temperature profile are derived from the power balance. They are compared with measurements and neoclassical predictions from the DKES code [5]. For both discharges, the calculated ion temperature agrees with the measurements.

The neoclassical diffusivities in Fig. 4 are total energy fluxes divided by the temperature gradients, hence the same quantity which is extracted from the power balance. In case of the ECH discharge,  $\chi$  agrees well with the neoclassical estimate for the ions and is well above the electron value. Hence, if the ions behave

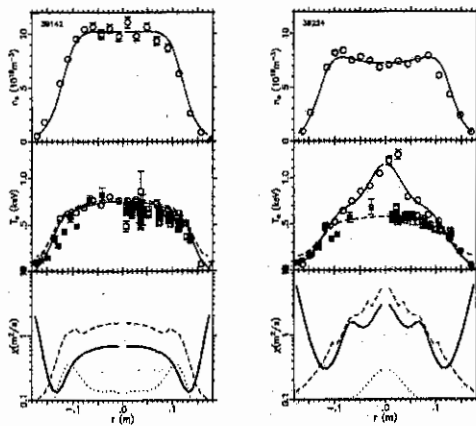


Fig. 4: Comparison of power balance analyses of a high-confinement NBI discharge (left) with an ECH discharge (right). Thomson electron density and temperature (open circles) and fits (solid lines), ion temperature as result from the power balance (dashed lines in the middle) and from charge-exchange spectroscopy (solid squares) and neutral particle analysis (open squares). Heat diffusivity from the power balance (solid line) compared to the equivalent neoclassical estimates for electrons (dotted) and ions (dashed).

neoclassically, the electron heat diffusivity must be strongly anomalous.

In case of the NBI discharge, there is an overall reduction of the diffusivity.  $\chi$  is below the neoclassical ion diffusivity and touches at its minimum the neoclassical electron diffusivity. From this result for  $\chi$  for  $r < 10$  cm, we cannot conclude that  $\chi_i$  is below the neoclassical value. A two fluid power balance showed that using the neoclassical prediction for  $\chi_i$  is also consistent with the central ion temperature measurements. In such an analysis in the core,  $\chi_e$  drops only by 20%. At the transport barrier ( $r \approx 12$  cm), however, the two fluid analysis fails to reproduce the data. Either the ion temperature is predicted as too high or, if in this region additional anomalous losses are added to the ion channel,  $\chi_e$  drops well below its neoclassical value. The result at the barrier is that either  $\chi_e$  or  $\chi_i$  or both are below the neoclassical prediction. Hence this region satisfies the criteria of a transport barrier in which anomalous transport seems to be suppressed.

**E × B and Magnetic Shear:** The slow temporal evolution of confinement could also point to current penetration and magnetic shear as an important ingredient. The  $\epsilon$  profile of the high-confinement NBI discharge has a low magnetic shear zone in the outer half of the plasma. By adding positive and negative currents to the discharge it was shown, that the magnetic shear was not the key parameter. It can be ruled out too that the existence of negative shear is, as in tokamaks, a pre-requisite of achieving the high confinement times.

In comparison with the transport barriers observed in the H-mode and in high performance tokamak discharges the role of the radial electric field is of special interest. In W7-AS in general, there is agreement between the electric field as deduced from spectroscopy and from the ambipolarity of the neoclassical fluxes [6]. Fig. 5 shows that this also holds for the high-confinement NBI discharges. The radial zone of low transport is characterized by strong gradients in the radial electric field and hence strong shear in the perpendicular plasma flow.

In Fig. 2, it was shown that the electric field increases together with electron and ion temperatures. The fact that confinement improves gradually rather than through a fast transition could point to a causality loop where transport is reduced by sheared flow generated by the neoclassical electric field. The reduction of transport steepens the gradients, which increase again the neoclassical electric field etc. This loop would stop when anomalous transport is suppressed and transport is on the neoclassical level. The time constants of the process would be in the order of the confinement time.

## References

- [1] KICK, M. et al., Proc. 16<sup>th</sup> Int. IAEA Conf., Montreal, 1996.
- [2] NAVE, M. F. F. et al., Nucl. Fusion **32** (1992) 825.
- [3] STROTH, et al., Nucl. Fusion **36** (1996) 1063.
- [4] BURHENN, R. et al., this conference.
- [5] MAASSBERG, H. et al., Phys. Fluids, **B5** (1993) 3627
- [6] BALDZUHN, J. et al., this conference.

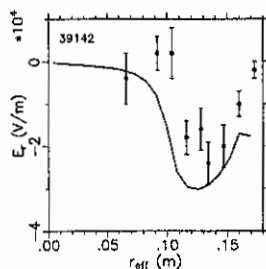


Fig. 5: Radial electric field as deduced from charge-exchange spectroscopy [6] and neoclassical theory.